Bioinspired Photo-crosslinking of Stretched Solid Silks for Enhanced Strength

Chang Liu†, Jiachuan Hua†, Pui Fai Ng†, Yidi Wang†, Bin Fei†, and Zhengzhong Shao‡*

† Institute of Textiles and Clothing, The Hong Kong Polytechnic University, Hong Kong, China

‡ Department of Macromolecular Science, Fudan University, Shanghai, China

* Corresponding author: tcfeib@polyu.edu.hk

ABSTRACT

In this study, solid fibroin fibers (FFs) were directly crosslinked by employing ruthenium-mediated redox pair under visible light at room temperature for the first time. The chemical crosslink through dityrosine connection was confirmed by FTIR, fluorescence spectra and solubility test. The resultant crosslink density in fibers was calculated based on their swelling ratio evaluation in LiBr solution. Further applying stretch to the fibers during irradiation improved the fiber strength to higher values. The break stress and Young's modulus of photo-crosslinked 15% stretch FFs reached 60%~90% increase in comparison to original FFs in dry and wet conditions. This approach constitutes an easy and straightforward strategy for strengthening FFs, which is scalable industrially to enhance FF in wide applications.

KEYWORDS: silk fibroin fiber; dityrosine; photo-crosslink; molecular orientation; strengthening

1. Introduction

Fibroin fiber (FF), produced by silk worm and then artificially purified by removing its sericin coating layer, has been widely applied in biomedical engineering as suture[1] and artificial implantable substitutes for ligament, tendon, nerve and vascular graft based on its biocompatibility in these cases.[2-5] It still suffers from an obvious weakening in a wet environment due to its water absorption tendency and unstable amorphous phase.[6] The stable strength of FFs in the wet state is of great interest to secure their application in body tissues by avoiding mechanical failure. Here we present a simple and general approach to alleviate this wet weakening problem in a green way.

Both physical and chemical methods have been reported to enhance silk fibroin strength. In physical way, several parameters, including solvents / salts, pH and temperature, were adjusted to modulate the silk fibroin crystallinity and mechanical strength.[7-9] Simply increasing the fibroin crystallinity usually makes the solid brittle, although raises its strength in some degree.[10] Forced stretching was proved to strengthen FFs via chain orientation.[11] The resultant FFs may still lose this orientation and strengthening effect in a wet condition. Chemical crosslinkers such as genipin and glutaraldehyde were employed to successfully enhance the mechanical strength of silk fibroin.[12,13] However, these chemical processes are time-consuming or cytotoxic, thus very limited in biomedical applications.[12,14] A rapid and mild chemical crosslink method is still in demand.

Dityrosine crosslinks have been detected in native elastic proteins in numerous structural tissues of insects, such as ligament resilin of locust, wing tedon of dragonfly, and aquatic silks of caddisflies.[15-17] Although those researchers did not directly explore the correlation between the

dityrosine crosslink and protein tensile property, we believe this crosslink is essential to realize the protein strength in forcing activity of living insects. Dityrosine and trityrosine linkages were also found in wild Tussah silk fibroin, but not in Bombyx mori silk, although both of them contain similar content of tyrosine unit. To our understanding, Bombyx mori silkworm has been domestically cultured for thousands of years in China, during which the cocoon whiteness is always favoured over the strength stability in harsh environment. This human selection has driven the Bombyx mori silkworm into an evolution route different from that of Tussah silkworm living in wild field. Suppose the insect ligaments/tedons or silkworm protective cocoons lost their strength (or obviously weakened) by water/moisture absorption, how do they survive near a river/pond or in a raining season? Inspired by the moisture-resistant stable strength of those dityrosine crosslinked structural tissues of wild insects, we aim to prepare dityrosine crosslink in the amorphous regions of Bombyx mori silk fibroin.

Chemical strategy of dityrosine link formation has been employed to fabricate hydrogels from solutions of specific proteins such as rec1-resilin,[18] fibrinogen and silk fibroin,[19,20] but has not been executed in solid materials. FF contains ~5 mol% reactive tyrosine units, which exist mostly in amorphous phase and are ready to be oxidized in-situ by proper agents infused.[21] So, we propose to extend this bio-inspired chemistry to the solid FF modification using a mild photocatalyst. Ruthenium is a kind of visible light photocatalyst and has many advantages such as chemical stability in storage, long excited state lifetime and commercial availability. It works with persulfates at room temperature; the resulting oxidants are capable of oxidizing tyrosine units in silk fibroin to generate radicals for polymerization or crosslinking. Based on this photo-initiated crosslinking and strengthening of FFs, the successful result would be useful and encouraging to both biomaterial enhancement (like suture) and textile functionalization (like

wrinkle free).[22]

2. Experimental Section

2.1 Materials

Silk was supplied by Huasheng Industrial Co., China. All chemicals were used without further purification, including tris(2,2′-bipyridyl)dichlororuthenium(II) hexahydrate ($Ru(bpy)_3Cl_2 \cdot 6H_2O$, Ru-bpy, Sigma-Aldrich), lithium bromide (LiBr, ≥ 99%, Sigma-Aldrich) and ammonium persulfate (APS, 98%, VWR Co.).

2.2 Photo-crosslinking of Silk Fibroin Fibers

The raw silk was degummed by IR heating (AHIBA IR PRO, Datacolor) in sealed water at 120 ℃ for 90 min, with a liquor ratio of 40:1, then rinsed three times and dried at room temperature overnight to obtain FFs. FFs were immersed in the solution of 0.5 mM Ru-bpy and 10 mM APS for 60 min in darkness at room temperature. Then swollen FFs were picked out and exposed to CIE Standard Illuminant D65 (Intensity: 8 W/m^2) for different periods (0~180 min) at 0~15% strains on a precision translation stage (TS304, Beijing Optical Century Instrument Co.) (Figure 1). Finally, the resultant FFs were rinsed by distilled water thoroughly and dried at 60 ℃ overnight.

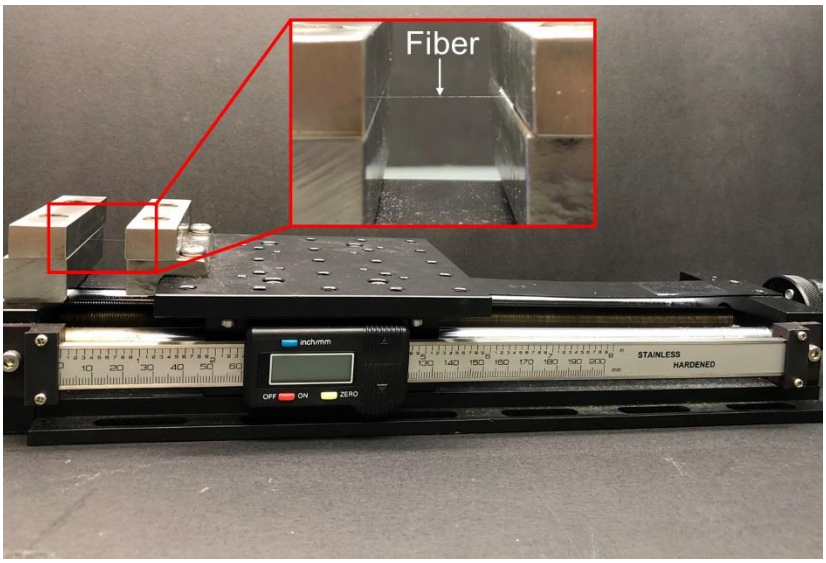

Figure 1. The photograph of swollen FFs on a precision translation stage device.

2.3 Characterization

FF samples were immersed in a pool of 9.3 M LiBr solution sandwiched between two glass slides at 65 °C for 30 min, and observed under an optical microscope (OPTIPHOT-POL, Nikon) to assess their solubility. The insoluble FFs were further immersed into excessive 9.3 M LiBr solution at 65 °C for 24 h, then filtered and recorded their wet mass ($W_{T,s}$). Then residues were washed with distilled water and dried at 60 °C to constant weight (W_p). The gel fraction (%) and swelling capacity (Q) were calculated by the following equations: gel fraction = W_p / W_i x 100%, Q = ($W_{T,s}$ - W_p) / W_p, where W_i was the initial weight of dry FF sample.

The fibroin volume fraction in fully swollen gel ($v_{1,s}$) was calculated from the Q value, using the density values of fibroin (ρ_p, taken as 1.421 g/cm^3) and LiBr solution (ρ_2, measured as 1.554 g/cm^3).[20] Crosslink density (v_e), the effective number of network junctions per unit volume (mol/cm^3), was calculated by the Flory-Rehner equation [23]

$$v_e = -\frac{\ln(1-v_{1,s})+v_{1,s}+\chi {v_{1,s}}^2}{\overline{v_2}({v_{1,s}}^{1/3}-\frac{1}{2}v_{1,s})} \quad (1)$$

where the Flory-Huggins interaction parameter (χ) was taken as 0.5,[24] and the molar volume of LiBr solution ($\overline{v_2}$) was calculated as 17.92 cm^3/mol. The number average molecular weight between crosslinks (M_c) was determined using the following equation

$$M_c = (v_e + \frac{2}{M_n})^{-1} \quad (2)$$

where the number average molecular weight of FFs (M_n) was taken as 390 kDa.[25]

Fourier-transform infrared spectra (FTIR) were acquired in the region of 4000-650 cm^{-1} with 16 scans at 4 cm^{-1} resolution (Spectrum 100, PerkinElmer). Fluorescence spectra were collected using a Spectrofluorometer FS5 excited at 330 nm. The stretch state for FFs was observed under polarizing microscope (DM2700M, Leica). The uniaxial tension test was operated by the Instron 4411 with a 10 N load cell and a gauge length of 20 mm, at a speed of 10 mm/min, where dry samples were standard conditioned at 25 ± 2 °C and relative humidity of 65 ± 5% for 24 h while wet samples were soaked in distilled water for 12 h before the test. FFs were also embedded in an epoxy resin (Historesin Embedding Kit, Leica) and sliced by microtome (RM2135, Leica) to obtain cross-sections. The FF cross-sectional areas were measured under a scanning electron microscope (SEM, VEGA3, Tescan operated at 20 kV) using the software 'Image J' by averaging 10 randomly chosen specimens.

2.4 Statistical Analysis

All test data were expressed as mean ± standard deviation (S.D.). Statistical significance was analysed by one-way analysis of variance (ANOVA) with post hoc Tukey testing. The *p* value less than 0.05 was considered to be statistically significant.

3. Results and Discussion

3.1 Solubility

As described in the experimental section, wet FFs containing Ru-bpy and APS were processed by visible light irradiation at room temperature. The sample irradiated for N min is recorded as photo-FF-N. The resultant FFs were assessed by solubility test in a highly concentrated LiBr solution. The original FF was confirmed as soluble in heated 9.3 M LiBr solution, as it lost most of its mass in 30 min (Figure 2a, 2c). At the same condition, the photo-FF-60 retained its integrity, was only swelled and expanded by 43.8% in diameter (Figure 2b, 2d). As hinted by this change in FF solubility, the photo-irradiation has successfully induced chemical crosslinking of FF with the Ru-bpy and APS, which worked as photocatalyst and oxidant. This crosslink is expected to occur at tyrosine unit, based on related literature works carried out in solutions.[26,27] Since tyrosine is rarely involved in fibroin crystal, dityrosine bonds would be formed in the amorphous regions of FFs via the photocatalytic reaction.

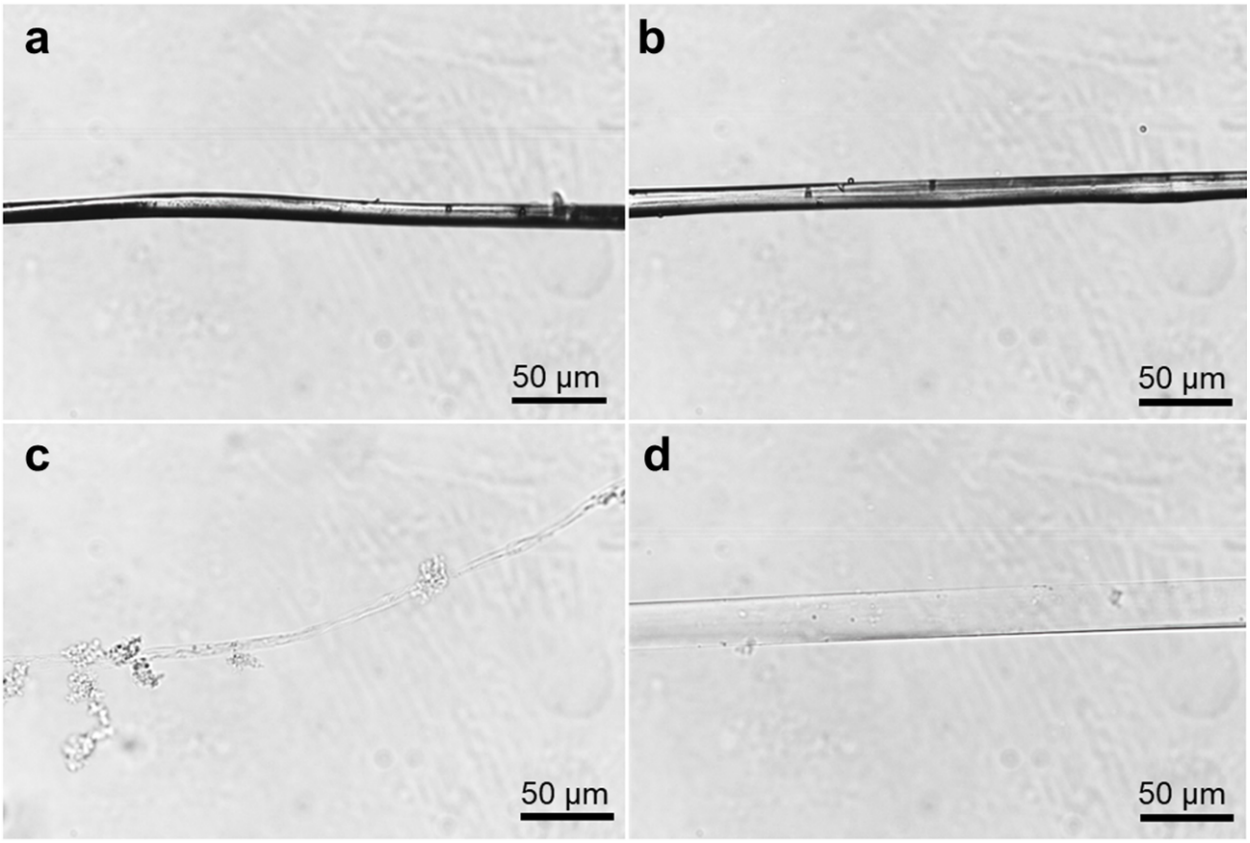

Figure 2. Microscope images of original FF (a) and photo-FF-60 (b), and their remnants in 9.3 M LiBr solution (65 °C for 30 min) (c and d).

3.2 Chemical Structure and Morphology

The FTIR and fluorescence spectra were used for studying the chemical change and secondary structure of original FFs and photo-crosslinked FF samples. From the FTIR results in Figure 3a, the original FF and photo-FF-60 samples exhibited the characteristic protein peaks at 1620 cm^{-1} (C=O stretching vibration, amide I), 1512 cm^{-1} (mainly N-H bending vibration, amide II) and 1228 cm^{-1} (mainly C-N stretching vibration, amide III).[28,29] In order to highlight the crosslink bond signal, we extracted the gel from crosslinked FFs by dissolution in an excessive 9.3 M LiBr solution. The gel from 'photo-FF-N' is defined as 'residue-N'. The peaks at 852 cm^{-1} and 826 cm^{-1}

were noticed in original FFs but significantly lowered in photo-FF-60 and residue-60, which were attributed to the aromatic C-H bending vibrations of tyrosine.[30-32] This change was caused by the reduction of aromatic C-H number after the coupling bonding between adjacent tyrosine groups.[20] The intensity of bands at 1331 and 1009 cm^{-1} prominently increased in the spectrum of residue-60, which were assigned to the stretching vibration mode of phenol C-O and the stretching vibration of dityrosine C-C bond, respectively. Hence, the dityrosine crosslink was produced in FFs with the Ru-bpy/APS redox system. For the residue-60 gel, the 1620 and 1512 cm^{-1} peaks changed in symmetricity and presented more fraction at high wavenumber side, indicating lower crystallinity due to the confinement of chain mobility by the dense crosslink.

Because tyrosine's characteristic fluorescence is sensitive to its chemical environment, we further measured the fluorescence spectra of several FF samples. As shown in Figure 3b, original FFs showed a fluorescence peak at 420 nm under 330 nm excitation, same as reported before.[33] Photo-FF-60 and residue-60 presented a wide fluorescence band with peak moved to 404 nm, confirming the formation of dityrosine.[17,34] The deconvoluted peak intensity ratio of I_{404}/I_{420} obviously increased with the increasing FF gel content (the peak fitting was completed with Origin graph software), where the 404 nm emission is attributed to the linked dityrosine structure while the 420 nm peak is assigned to the original tyrosine unit.

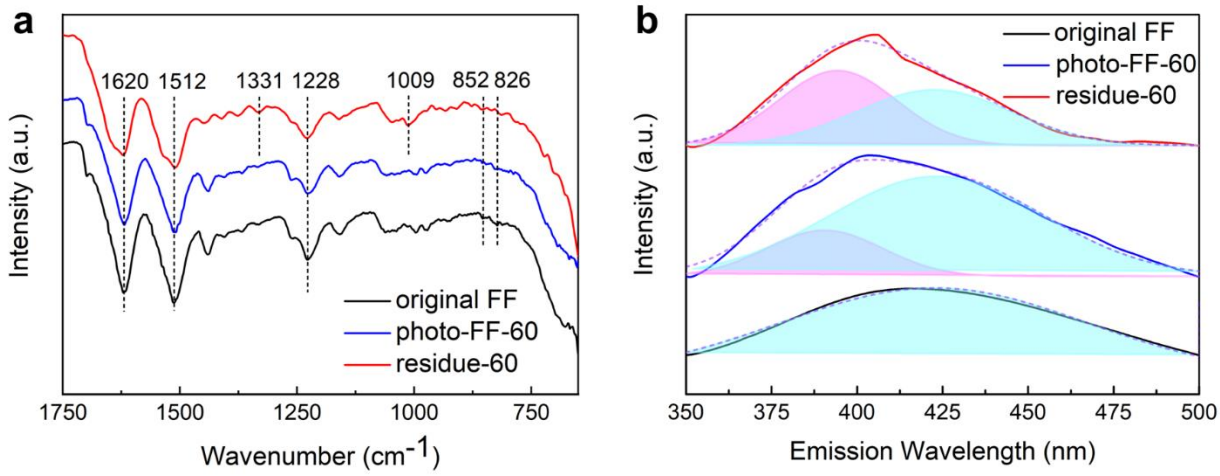

Figure 3. (a) FTIR and (b) fluorescence spectra excited at 330 nm of original FFs, photo-FF-60 and residue-60.

The original FFs showed weak UV-excited blue fluorescence while residue-60 showed bright blue fluorescence due to the presence of dityrosine (Figure 4a and 4b), which was consistent with the results of fluorescence spectra. Moreover, residue-60 displayed yellowish-brown color because of protein oxidation,[35] while original FFs did not offer any obvious shade. The surface morphologies of samples were observed under SEM after fully swelling and freeze-drying (freezer dryer, Beijing Boyikang Laboratory Instruments Co.). In their side view (Figure 4c-e), original FFs, photo-FF-60 and photo-FF-180 showed a smooth surface. However, residue-60 and residue-180 after swelling in LiBr solution presented flawed structure and significantly increased diameter by 158% and 71% (Figure 4f and 4g). Additionally, many regular grooves were noticed on the surfaces of residue samples due to the axial-directional shrinkage of fiber allowed by the increased protein mobility in its good solvent. Their cross-sections were also observed under SEM, which agreed with the above results and presented more obvious wrinkles on side surfaces (Figure 4c'-4g').

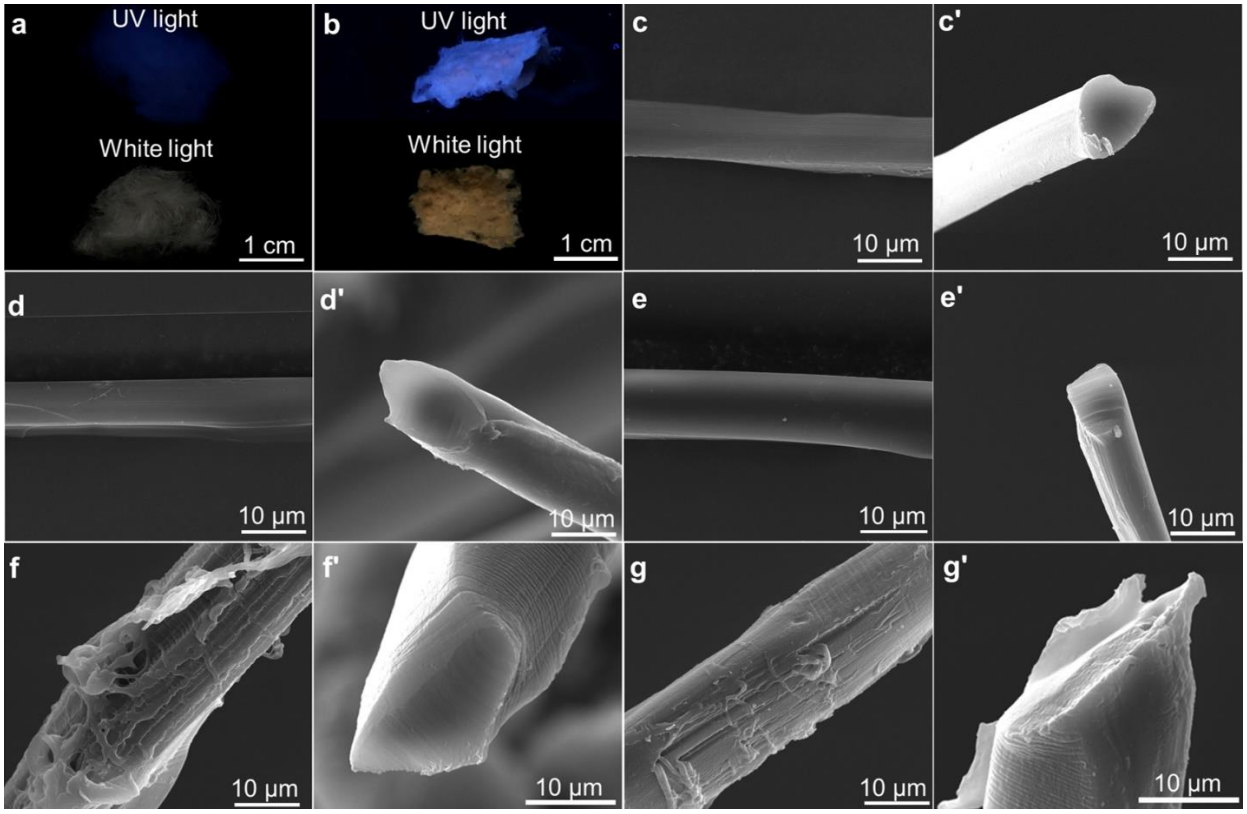

Figure 4. The photographs of original FFs (a) and residue-60 (b) under UV light and white light. SEM images of original FF (c), photo-FF-60 (d), photo-FF-180 (e), freeze-dried residue-60 (f) and residue-180 (g) after swelling in LiBr solution, where apostrophe (') indicates their corresponding cross-sections.

3.4 Crosslink Density

Taking 9.3 M LiBr solution at 65 °C as a good solvent for FF, the gel fractions of photo-FF-30, photo-FF-60 and photo-FF-180 were measured by solvent extraction as 9.21%, 37.7% and 35.1% in Table 1. Furthermore, the swelling values (Q_s) of residue-30, residues-60 and residues-180 were recorded as 47.03 g/g, 13.89 g/g and 14.03 g/g. Based on the Flory-Rehner equation, the crosslink density values (V_e) of residues -30, -60 and -180 were calculated as 8.17×10^{-7}, 2.01 ×

10^{-5}, and 1.96×10^{-5} mol/cm^3, respectively. To further evaluate the fraction of tyrosine crosslinked in FFs, the theoretical maximum value of crosslink density was calculated based on the number of tyrosine units in the heavy chain of silk fibroin.

The tyrosine units (5.3 mol%, 277 units) are available in the heavy chains of silk fibroin (Mn ~ 390 kDa, ρ_p = 1.421 g/cm^3),[36] which have an opportunity for dityrosine formation. When we assumed the tyrosine conversion ratio is 100%, the theoretical value of dityrosine crosslink density is approximately 5.05×10^{-4} mol/cm^3. Hence, the experimental crosslink density values of residue-30, residue-60 and residue-180 account for 0.16%, 3.98% and 3.88% of the theoretical maximum density, corresponding to the tyrosine conversion ratio of 0.16%, 3.98% and 3.88%. In a previous study, the conversion ratio of tyrosine to dityrosine was reported as 28-56% in synthesized silk fibroin hydrogels.[37] The crosslink density generated in reactions was affected by fibroin concentration, protein chain mobility, and nearby units.[37] Based on our results, FFs were regarded as an extremely high concentration of fibroin, where the chain mobility was low in solid crystalline state. The collisions between phenolic radicals on tyrosine units were limited by the low chain mobility, which resulted in the low crosslink yield in solid state reaction. What is the possible effect of such low crosslink density on the fiber tensile property?

Table 1. Network parameters determined from equilibrium swelling studies of photo-crosslinked FF samples in 9.3 M LiBr solution.

Sample	Gel fraction (%)	Q (g/g)	$v_{1,s}$	v_e (mol/cm^3)	M_c (g/mol)
residue-30	9.21	47.03	0.0227	8.17×10^{-7}	1.68×10^5

residue-60	37.7	13.89	0.0730	2.01×10^{-5}	3.97×10^{4}
residue-180	35.1	14.03	0.0723	1.96×10^{-5}	4.05×10^{4}

3.5 Mechanical Property

The representative stress-strain curves of original FFs and photo-crosslinked FFs were shown and analysed in Figure 5a, 5b. In comparison to original FFs, the photo-FF-30 did not show obvious change in break stress (from 313 ± 45 MPa to 315 ± 51 MPa), but presented evident increment in Young's modulus (from 6.57 ± 0.76 GPa to 8.01 ± 0.66 GPa). With the increase of irradiation time, the break stress increased to 359 ± 36 MPa (photo-FF-60) and 373 ± 48 MPa (photo-FF-120), and the Young's modulus also rose to 8.08 ± 0.60 GPa (photo-FF-60) and 8.47 ± 0.88 GPa (photo-FF-120). However, when the irradiation time was further extended to 180 min, the break stress and the Young's modulus decreased to 354 ± 49 MPa and 7.71 ± 0.84 GPa for photo-FF-180. The longer time irradiation caused little improvement in strength and modulus due to the limited amount of applied oxidants and free tyrosine units, where the negative effect of irradiation (e.g., degradation of FFs) surpassed the positive impact of crosslinking on tensile properties. Furthermore, the elongation at break was around 15% for original and photo-crosslinked FF samples despite some fluctuations (within 10%). Take an overview on the irradiation treatment, the break stress and Young's modulus of photo-crosslinked FFs increased with time at beginning and started to decline after 120 min, while the maximum elongation was stable with slight fluctuation. Irradiation 60 min was the optimal period and generated 15% and 23% increment in break stress and Young's modulus by dityrosine linkage, although the corresponding crosslink percentage of total tyrosine units was less than 5%.[21] This condition was used for the following stretch process of FFs.

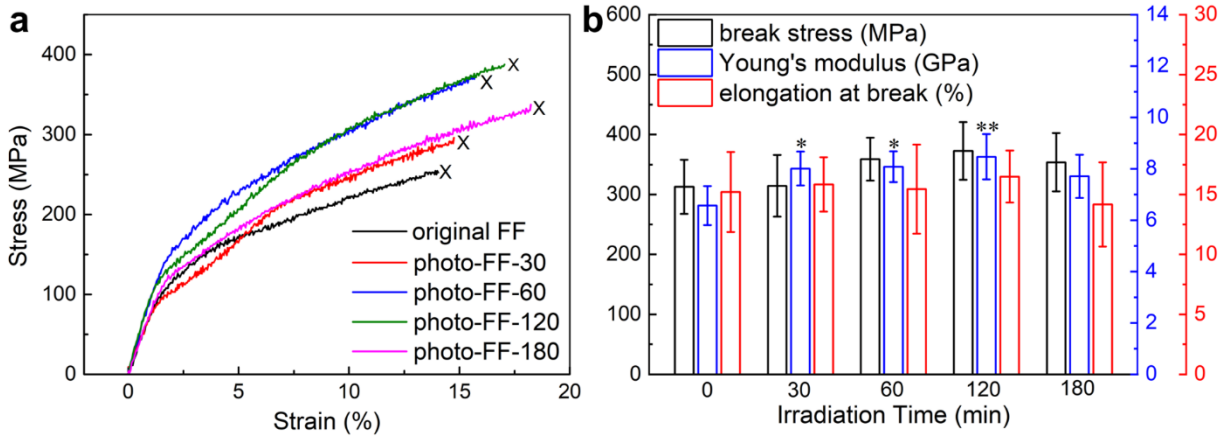

Figure 5. (a) The representative stress-strain curves and (b) break stress, Young's modulus and elongation at break of FFs under various irradiation periods. *p < 0.05, **p < 0.01 compared with the original FF group.

In order to further increase the tensile strength of FFs, we also tried the irradiation of FFs under stretch deformation. When the FF was stretched under polarizing microscope, its diameter reduction and color shift to blue were clearly observed, indicating the protein orientation in both crystalline and amorphous regions by stretch (Figure 6).[38] This molecular orientation was expected to cause an increment in tensile strength. After the irradiation of FFs under different stretches, their cut cross-sections were observed under SEM in relaxed state. The obtained cross-section areas of FFs became smaller with increasing stretch ratio, indicating the reserved stretch deformation and remaining molecular orientation in FFs (Figure 8a, S1). These photo-crosslinked FFs were tested in tensile property again, with representative stress-strain curves shown in Figure 7a. The sample irradiated for 60 min under N% stretch is recorded as photo-FF-N%. With the stretch ratio increasing to 5%, 10% and 15%, the break stress of FFs increased to

442 ± 68, 482 ± 74, and 514 ± 26 MPa respectively; meanwhile, their Young's modulus increased to 8.56 ± 0.92, 9.23 ± 0.76, and 10.62 ± 0.85 GPa respectively (Figure 7c, 7d). The downward trend in the maximum elongation of stretched FF samples also revealed both crystalline and amorphous region deformations occurred in fibers when the stretch was executed (Figure 7e). The decrement in maximum elongation was mainly caused by the molecular orientation within the amorphous region and the alignment of scattered crystals along the fiber axis in stretch. Comparing to original FF, photo-FF-15% presented 64% and 62% increment in break stress and Young's modulus respectively, while 19% decrement in the maximum elongation. These results are comparable to the values reported in literature for artificially stretched FFs.[11]

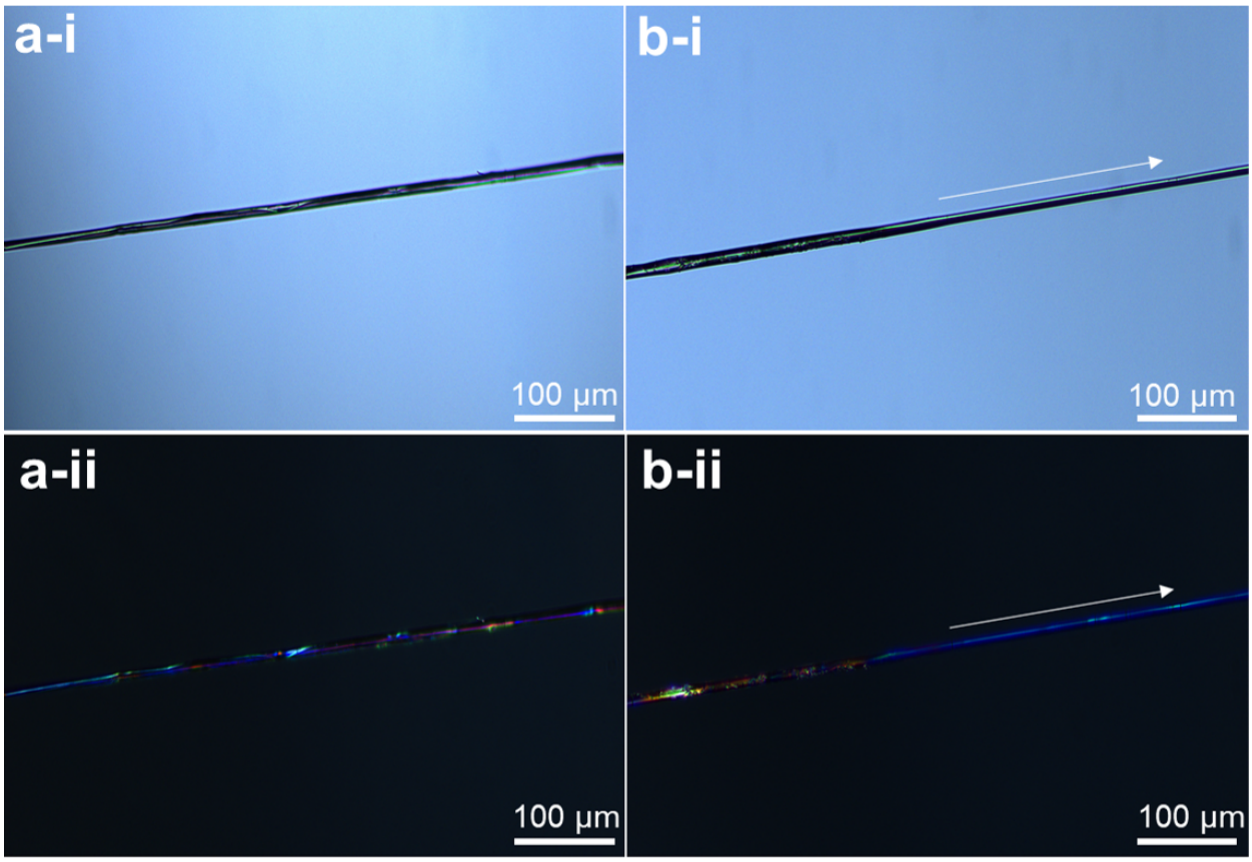

Figure 6. Polarizing microscope images of the FF in relaxed (a) and stretched (b) states under parallel (i) and crossed (ii) polarizers (formic acid droplet).

As mentioned at the beginning, this work targeted at wet weakening problem of silk. Our photo-initiated crosslink was expected to retain the FF strength in wet condition, through limiting the water lubricating effect among amorphous chain segments. The representative stress-strain curves of wet FFs were shown in Figure 7b, with their break stress and modulus values shown in Figure 7c, 7d. In the view of break stress, the crosslinked FFs presented obviously less reduction after getting fully wetted. These reduction percentages of wet fibers were calculated and demonstrated in Figure 8b. The trend of break stress of photo-crosslinked stretched samples in the wet condition was also presented in Figure 7c. Wetting resulted in an obvious reduction in fiber strength, because hydrogen bonds between proteins easily dissociated in water. The covalent crosslink was able to limit the movement of molecular chains and resistant to water infusion. Hence, the break stress of photo-FF-60 showed a minimum decline (2%) in the wet condition. The photo-crosslinked 5~15% stretch samples indicated a 5~10% break stress decline compared to those in dry condition, while original FFs showed an 18% decrease because of the rareness of crosslink inside the fiber. The break stress decrease of these photo-crosslinked stretched samples was possibly caused by the partial loss of the molecular orientation with residual stress upon wetting. A higher stretch (e.g., 50% stretch) is likely to provide more promising strength enhancement, but the current photo-FF-15% also exhibited a significant increment (over 90%) of the break stress against original FFs in the wet condition, which hinted broad prospect of application. On the other hand, the Young's modulus of FF samples in the wet condition decreased more evidently in Figure 7d, 8b, because water molecule acted as plasticizer

for fibers. However, the Young's modulus of photo-FF-15% still behaved 66% higher than original FFs in wet condition and comparable to the original dry FFs. The elongation at break in the wet state also indicated the movement of molecular chain in fibers as shown in Figure 7e. The disruption of hydrogen bonds between proteins resulted in the swelling of fibers and enhanced the flexibility of protein chains, leading to a nearly 30% increment in elongation at break of original FFs (Figure 8c). However, the maximum elongation of photo-crosslinked FFs fluctuated slightly, especially photo-crosslinked stretched FF samples (2~7%). The almost unchanged elongation at break for photo-crosslinked stretched FFs in dry and wet states exhibited the low flexibility of protein chains and effective fixation of molecular orientation in FFs by stretch and crosslink (Figure 8c). These photo-crosslinked stretch FFs still showed remarkable tensile strength in the wet condition, superior to the silks generated by other technologies as shown in Figure 7f.[6,40-43] Therefore, this stretch during photo irradiation was confirmed effective to further increase the tensile property of crosslinked FFs in both dry and wet conditions.

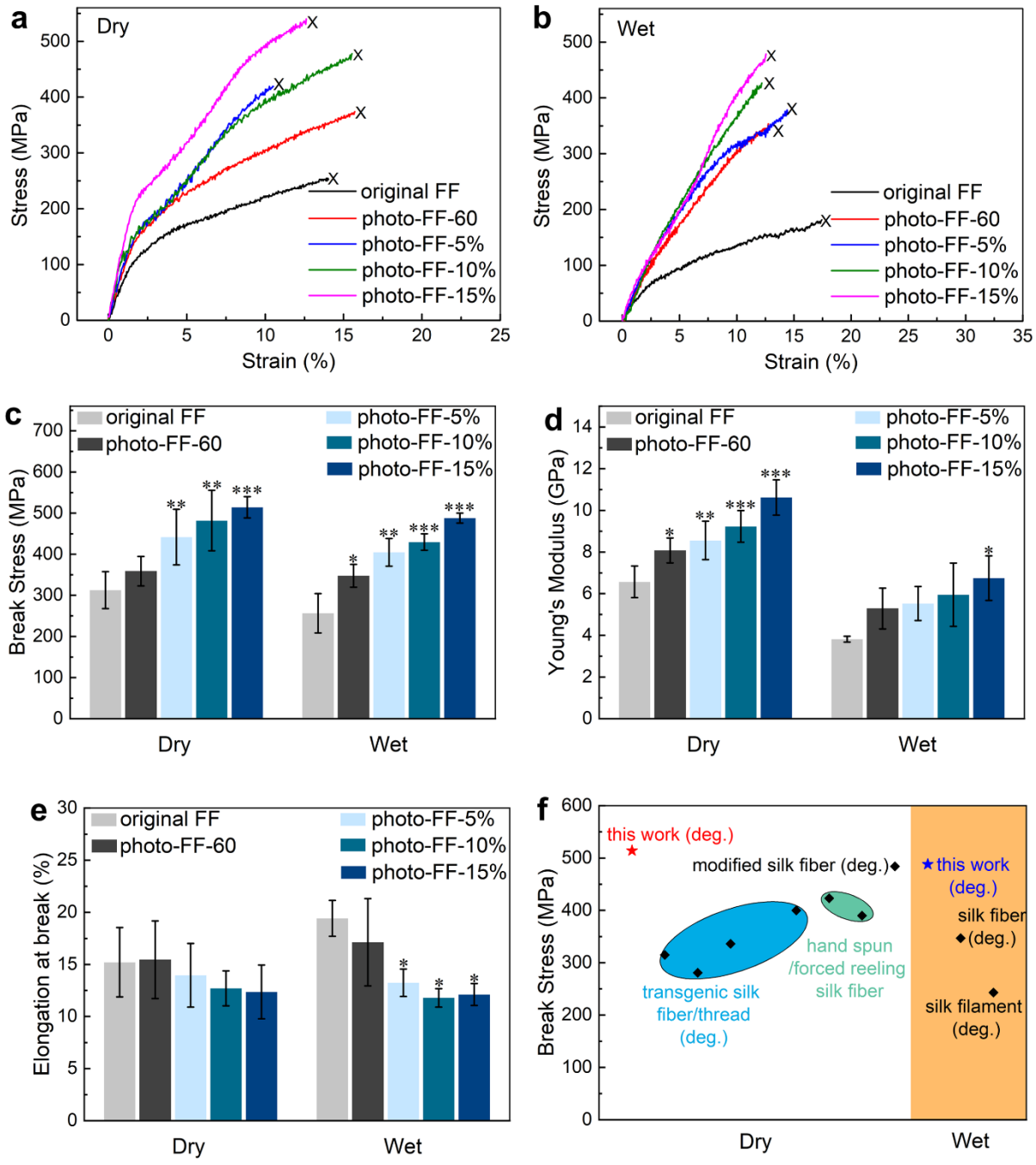

Figure 7. (a, b) Representative stress-strain curves, (c) break stress, (d) Young's modulus and (e) elongation at break of original FFs and photo-crosslinked FFs under different stretches in dry and wet conditions. *$p < 0.05$, **$p < 0.01$, ***$p < 0.001$ compared with the original FF group in either dry or wet conditions. (f) Comparison in break stress values of silk fibers modified by

different technologies including transgene,[39,40] forced silking[6,41] and gelatin-modification[42], as well as break stress of silk materials in the wet state[6,43] (deg: degummed).

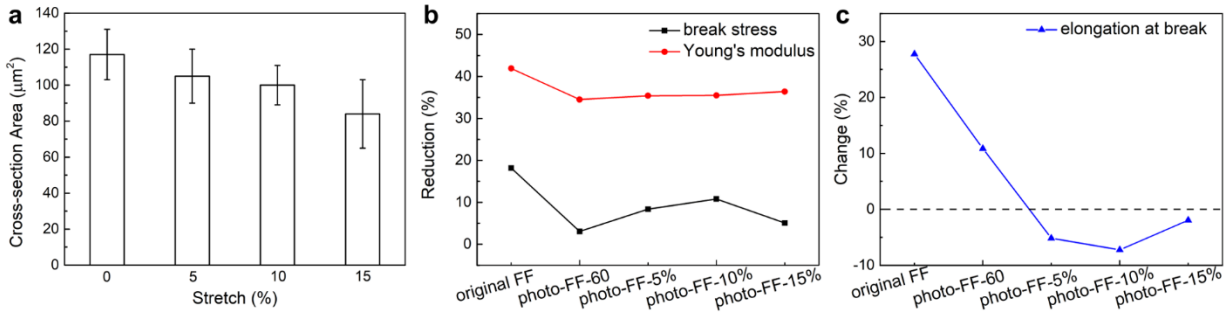

Figure 8. (a) The cross-section areas of photo-crosslinked FFs under different stretches. The change percentage of (b) FFs' break stress, Young's modulus and (c) elongation at break after they were fully wetted.

In summary, the tensile strength of FFs was progressively improved by the combination of molecular orientation and dityrosine linkages. As illustrated in Figure 9, the FFs were firstly stretched in the solution of Ru-bpy and APS to enrich the fibers with necessary chemicals and molecular orientation, then irradiated under white light to achieve chemical crosslink via dityrosine bond formation. The resultant photo-FF-15% presented significantly increased break stress, which was 64% and 90% higher than those of original FFs in dry and wet conditions. Moreover, the Young's modulus of photo-FF-15% behaved 62% and 66% higher than original FFs in dry and wet conditions. Therefore, robust solid FFs were successfully fabricated by the approach of photo-crosslinking in stretch.

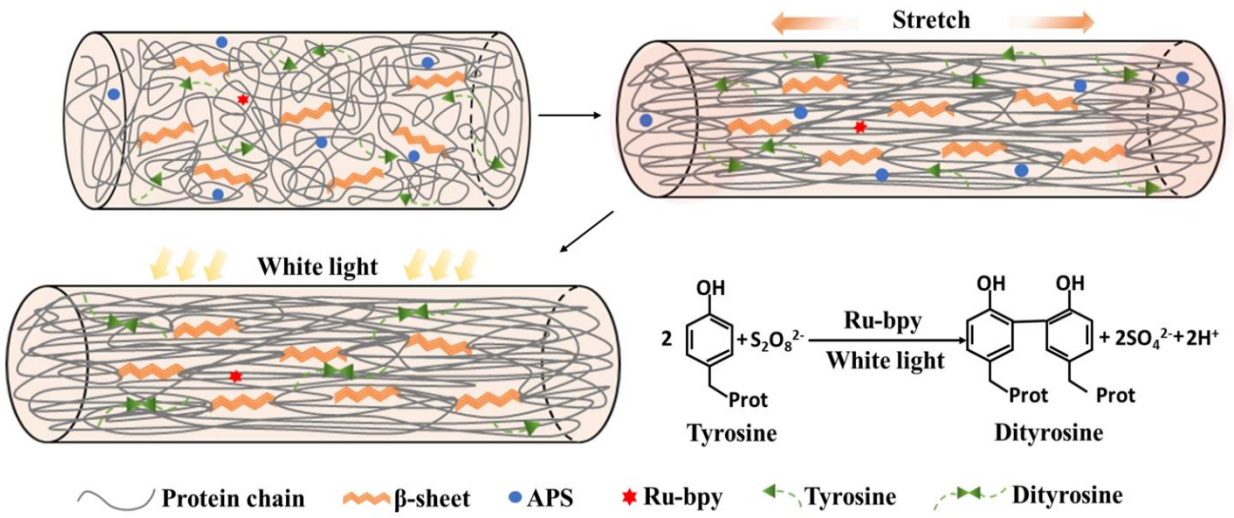

Figure 9. Schematic of the stretched and photo-crosslinked FF showing molecular orientation and dityrosine linkage.

4. Conclusions

In conclusion, the dityrosine crosslink was successfully prepared in FFs by ruthenium-mediated photo-crosslink method under visible light at room temperature. The occurrence of dityrosine in FFs was confirmed by FTIR, fluorescence spectra and solubility test. Furthermore, the break stress and Young's modulus of photo-crosslinked 15% stretch FFs were significantly increased by 64% and 62% in the dry condition, and by 90% and 66% in the wet condition compared with original FFs, due to the improvement of molecular orientation by stretch and the formation of dityrosine linkage. The approach of photo-crosslinking in stretch contributed to the strength boosting of FFs. This work is the first success to crosslink solid FFs in stretch via tyrosine units, highlighting potential applications in wide engineering fields.

ASSOCIATED CONTENT

Supporting Information.

The following files are available free of charge.

Cross-sectional SEM images of photo-FF-60, photo-FF-5%, photo-FF-10% and photo-FF-15%. (PDF)

AUTHOR INFORMATION

Corresponding Author

*Bin Fei − Institute of Textiles and Clothing, The Hong Kong Polytechnic University, Hong Kong, China; Email: tcfeib@polyu.edu.hk

Author Contributions

The manuscript was written through contributions of all authors. All authors have given approval to the final version of the manuscript.

Notes

The authors declare no competing financial interest.

ACKNOWLEDGMENT

We thank the support of General Research Fund PolyU152156/17E from Hong Kong Research Grant Council and the matching fund G-YBRF from Hong Kong Polytechnic University.

REFERENCES

(1) Baygar, T.; Sarac, N.; Ugur, A.; Karaca, I. R., Antimicrobial characteristics and biocompatibility of the surgical sutures coated with biosynthesized silver nanoparticles. *Bioorg. Chem.* **2019,** 86, 254-258.

(2) Altman, G. H.; Horan, R. L.; Lu, H. H.; Moreau, J.; Martin, I.; Richmond, J. C.; Kaplan, D. L., Silk matrix for tissue engineered anterior cruciate ligaments. *Biomaterials* **2002**, 23 (20), 4131-4141.

(3) Kwon, S.-Y.; Chung, J.-W.; Park, H.-J.; Jiang, Y.-Y.; Park, J.-K.; Seo, Y.-K., Silk and collagen scaffolds for tendon reconstruction. *Proc. Inst. Mech. Eng., Part H* **2014**, 228 (4), 388-396.

(4) Pillai, M. M.; Sathishkumar, G.; Houshyar, S.; Senthilkumar, R.; Quigley, A.; Shanthakumari, S.; Padhye, R.; Bhattacharyya, A., Nanocomposite-coated silk-based artificial conduits: The influence of structures on regeneration of the peripheral nerve. *ACS Appl. Bio Mater.* **2020**, 3 (7), 4454-4464.

(5) Kiritani, S.; Kaneko, J.; Ito, D.; Morito, M.; Ishizawa, T.; Akamatsu, N.; Tanaka, M.; Iida, T.; Tanaka, T.; Tanaka, R., Silk fibroin vascular graft: a promising tissue-engineered scaffold material for abdominal venous system replacement. *Sci. Rep.* **2020**, 10 (1), 1-9.

(6) Colomban, P.; Dinh, H. M.; Bunsell, A.; Mauchamp, B., Origin of the variability of the mechanical properties of silk fibres: 1 - The relationship between disorder, hydration and stress/strain behaviour. *J. Raman Spectrosc.* **2012**, 43 (3), 425-432.

(7) Ng, P. F.; Lee, K. I.; Meng, S.; Zhang, J.; Wang, Y.; Fei, B., Wet Spinning of Silk Fibroin-Based Core–Sheath Fibers. *ACS Biomater. Sci. Eng.* **2019,** 5 (6), 3119-3130.

(8) Xiao, L. Y.; Liu, S. S.; Yao, D. Y.; Ding, Z. Z.; Fan, Z. H.; Lu, Q.; Kaplan, D. L., Fabrication of Silk Scaffolds with Nanomicroscaled Structures and Tunable Stiffness. *Biomacromolecules* **2017,** 18 (7), 2073-2079.

(9) Hu, X.; Shmelev, K.; Sun, L.; Gil, E. S.; Park, S. H.; Cebe, P.; Kaplan, D. L., Regulation of silk material structure by temperature-controlled water vapor annealing. *Biomacromolecules* **2011,** 12 (5), 1686-1696.

(10) de Moraes, M. A.; Weska, R. F.; Beppu, M. M., Effects of sterilization methods on the physical, chemical, and biological properties of silk fibroin membranes. *J. Biomed. Mater. Res. Part B* **2014,** 102 (4), 869-876.

(11) Beth Mortimer, Juan Guan, Chris Holland, David Porter, Fritz Vollrath. Linking naturally and unnaturally spun silks through the forced reeling of Bombyx mori. *Acta Biomater.* **2015**, 11, 247–255.

(12) Vasconcelos, A.; Gomes, A. C.; Cavaco-Paulo, A., Novel silk fibroin/elastin wound dressings. *Acta Biomater.* **2012,** 8 (8), 3049-3060.

(13) Zhu, B.; Li, W.; Chi, N.; Lewis, R. V.; Osamor, J.; Wang, R., Optimization of Glutaraldehyde Vapor Treatment for Electrospun Collagen/Silk Tissue Engineering Scaffolds. *ACS Omega* **2017,** 2 (6), 2439-2450.

(14) Liu, C.; Hua, J.; Ng, P. F.; Fei, B., Photochemistry of bioinspired dityrosine crosslinking. *J. Mater. Sci. Technol.* **2021,** 63, 182-191.

(15) Andersen, S. O., Characterization of a new type of cross-linkage in resilin, a rubber-like protein. *Biochim. Biophys. Acta* **1963**, 69, 249-262.

(16) Andersen, S. O., The cross-links in resilin identified as dityrosine and trityrosine. *Biochim. Biophys. Acta, Gen. Subj.* **1964**, 93 (1), 213-215.

(17) Partlow, B. P.; Applegate, M. B.; Omenetto, F. G.; Kaplan, D. L., Dityrosine Cross-Linking in Designing Biomaterials. *ACS Biomater. Sci. Eng.* **2016**, 2 (12), 2108-2121.

(18) Truong, M. Y.; Dutta, N. K.; Choudhury, N. R.; Kim, M.; Elvin, C. M.; Nairn, K. M.; Hill, A. J., The effect of hydration on molecular chain mobility and the viscoelastic behavior of resilin-mimetic protein-based hydrogels. *Biomaterials* **2011,** 32 (33), 8462-8473.

(19) Elvin, C. M.; Brownlee, A. G.; Huson, M. G.; Tebb, T. A.; Kim, M.; Lyons, R. E.; Vuocolo, T.; Liyou, N. E.; Hughes, T. C.; Ramshaw, J. A.; Werkmeister, J. A., The development of photochemically crosslinked native fibrinogen as a rapidly formed and mechanically strong surgical tissue sealant. *Biomaterials* **2009,** 30 (11), 2059-2065.

(20) Whittaker, J. L.; Choudhury, N. R.; Dutta, N. K.; Zannettino, A., Facile and rapid ruthenium mediated photo-crosslinking of Bombyx mori silk fibroin. *J. Mater. Chem. B* **2014,** 2 (37), 6259-6270.

(21) Kim, C. S.; Yang, Y. J.; Bahn, S. Y.; Cha, H. J., A bioinspired dual-crosslinked tough silk protein hydrogel as a protective biocatalytic matrix for carbon sequestration. *NPG Asia Mater.* **2017,** 9 (6), e391.

(22) Lee, K. I.; Wang, X.; Guo, X.; Yung, K. F.; Fei, B., Highly water-absorbing silk yarn with interpenetrating network via in situ polymerization. *Int. J. Biol. Macromol.* **2017,** 95, 826-832.

(23) Lin, H. Q.; Kai, T.; Freeman, B. D.; Kalakkunnath, S.; Kalika, D. S., The effect of cross-linking on gas permeability in cross-linked poly(ethylene glycol diacrylate). *Macromolecules* **2005,** 38 (20), 8381-8393.

(24) Mark, J. E., *Physical properties of polymers handbook*. Springer: 2007, pp 233-234.

(25) Inoue, S.; Tanaka, K.; Arisaka, F.; Kimura, S.; Ohtomo, K.; Mizuno, S., Silk fibroin of Bombyx mori is secreted, assembling a high molecular mass elementary unit consisting of H-chain, L-chain, and P25, with a 6:6:1 molar ratio. *J. Biol. Chem.* **2000,** 275 (51), 40517-40528.

(26) Min, K. I.; Kim, D. H.; Lee, H. J.; Lin, L.; Kim, D. P., Direct Synthesis of a Covalently Self-Assembled Peptide Nanogel from a Tyrosine-Rich Peptide Monomer and Its Biomineralized Hybrids. *Angew. Chem. Int. Ed.* **2018,** 57 (20), 5630-5634.

(27) Kim, I.; Bang, W. Y.; Park, W. H.; Han, E. H.; Lee, E., Photo-crosslinkable elastomeric protein-derived supramolecular peptide hydrogel with controlled therapeutic CO-release. *Nanoscale* **2019,** 11 (37), 17327-17333.

(28) Barth, A., The infrared absorption of amino acid side chains. *Prog. Biophys. Mol. Biol.* **2000,** 74 (3-5), 141-173.

(29) Boulet-Audet, M.; Lefevre, T.; Buffeteau, T.; Pezolet, M., Attenuated total reflection infrared spectroscopy: An efficient technique to quantitatively determine the orientation and conformation of proteins in single silk fibers. *Appl. Spectrosc.* **2008,** 62 (9), 956-962.

(30) Sampaio, S.; Taddei, P.; Monti, P.; Buchert, J.; Freddi, G., Enzymatic grafting of chitosan onto Bombyx mori silk fibroin: kinetic and IR vibrational studies. *J. Biotechnol.* **2005,** 116 (1), 21-33.

(31) Sirichaisit, J.; Brookes, V. L.; Young, R. J.; Vollrath, F., Analysis of structure/property relationships in silkworm (Bombyx mori) and spider dragline (Nephila edulis) silks using Raman Spectroscopy. *Biomacromolecules* **2003,** 4 (2), 387-394.

(32) Winnard, P. T.; Zhang, C.; Vesuna, F.; Kang, J. W.; Garry, J.; Dasari, R. R.; Barman, I.; Raman, V., Organ-specific isogenic metastatic breast cancer cell lines exhibit distinct Raman spectral signatures and metabolomes. *Oncotarget* **2017,** 8 (12), 20266-20287.

(33) Cavallini, S.; Toffanin, S.; Chieco, C.; Sagnella, A.; Formaggio, F.; Pistone, A.; Posati, T.; Natali, M.; Caprini, M.; Benfenati, V.; Di Virgilio, N.; Ruani, G.; Muccini, M.; Zamboni, R.; Rossi, F., Naturally functionalized silk as useful material for photonic applications. *Composites, Part B* **2015,** 71, 152-158.

(34) Min, K. I.; Yun, G.; Jang, Y.; Kim, K. R.; Ko, Y. H.; Jang, H. S.; Lee, Y. S.; Kim, K.; Kim, D. P., Covalent Self-Assembly and One-Step Photocrosslinking of Tyrosine-Rich Oligopeptides to Form Diverse Nanostructures. *Angew. Chem. Int. Ed.* **2016,** 55 (24), 6925-6928.

(35) Freddi, G.; Anghileri, A.; Sampaio, S.; Buchert, J.; Monti, P.; Taddei, P., Tyrosinase-catalyzed modification of Bombyx mori silk fibroin: grafting of chitosan under heterogeneous reaction conditions. *J. Biotechnol.* **2006,** 125 (2), 281-294.

(36) Murphy, A. R.; Kaplan, D. L., Biomedical applications of chemically-modified silk fibroin. *J. Mater. Chem.* **2009,** 19 (36), 6443-6450.

(37) McGill, M.; Coburn, J. M.; Partlow, B. P.; Mu, X.; Kaplan, D. L., Molecular and macro-scale analysis of enzyme-crosslinked silk hydrogels for rational biomaterial design. *Acta Biomater.* **2017,** 63, 76-84.

(38) Hong, K.; Strobl, G., Network stretching during tensile drawing of polyethylene: a study using X-ray scattering and microscopy. *Macromolecules* **2006,** 39 (1), 268-273.

(39) Teule, F.; Miao, Y. G.; Sohn, B. H.; Kim, Y. S.; Hull, J. J.; Fraser, M. J., Jr.; Lewis, R. V.; Jarvis, D. L., Silkworms transformed with chimeric silkworm/spider silk genes spin

composite silk fibers with improved mechanical properties. *PNAS USA* **2012**, 109 (3), 923-8.

(40) Hiramatsu, S.; Moriyama, H.; Asaoka, R.; Morita, K.; Tanaka, T.; Yamada, K.; Obrien, J. P.; Fahnestock, S. R., Silk Thread Containing Spider Thread Protein and Silk Worm Producing the Silk Thread. *US Pat.* **2008**.

(41) Mortimer, B.; Holland, C.; Vollrath, F., Forced reeling of Bombyx mori silk: separating behavior and processing conditions. *Biomacromolecules* **2013**, 14 (10), 3653-9.

(42) Liu, H.; Ge, Z.; Wang, Y.; Toh, S. L.; Sutthikhum, V.; Goh, J. C., Modification of sericin-free silk fibers for ligament tissue engineering application. *J Biomed. Mater. Res. B Appl. Biomater.* **2007**, 82 (1), 129-38.

(43) Chattopadhyay, S. D. R.; Gulrajani, M.; Sen, K., Study of property and structural variants of mulberry and tasar silk filaments. *Autex Res. J.* **2005**, 5, 81-86.

For Table of Contents Use Only

Bioinspired Photo-crosslinking of Stretched Solid Silks for Enhanced Strength

Chang Liu†, Jiachuan Hua†, Pui Fai Ng†, Yidi Wang†, Bin Fei†, and Zhengzhong Shao‡*

† Institute of Textiles and Clothing, The Hong Kong Polytechnic University, Hong Kong, China

‡ Department of Macromolecular Science, Fudan University, Shanghai, China

* Corresponding author: tcfeib@polyu.edu.hk